Catalysts **2015**, *5*, 2271-2286; doi:10.3390/catal5042271

OPEN ACCESS

catalysts

ISSN 2073-4344

www.mdpi.com/journal/catalysts

Article

Washcoat Deposition of Ni- and Co-ZrO_2 Low Surface Area Powders onto Ceramic Open-Cell Foams: Influence of Slurry Formulation and Rheology

Riccardo Balzarotti *, Mirko Ciurlia †, Cinzia Cristiani † and Fabio Paparella †

Politecnico di Milano, Dipartimento di Chimica, Materiali e Ingegneria Chimica "G. Natta", Piazza Leonardo da Vinci 32, 20133 Milano, Italy; E-Mails: mirko.ciurlia@mail.polimi.it (M.C.); cinzia.cristiani@polimi.it (C.C.); fabio.paparella@mail.polimi.it (F.P.)

† These authors contributed equally to this work.

* Author to whom correspondence should be addressed; E-Mail: riccardo.balzarotti@polimi.it; Tel.: +39-02-2399-3232; Fax: +39-02-2399-3180.

Academic Editor: Keith Hohn

Received: 29 September 2015 / Accepted: 24 November 2015 / Published: 18 December 2015

Abstract: The effect of formulations and procedures to deposit thin active layers based on low surface area powders on complex geometry substrates (open-cell foams) was experimentally assessed. An acid-free liquid medium based on water, glycerol, and polyvinyl alcohol was used for powder dispersion, while a dip-coating technique was chosen for washcoat deposition on 30 PPI ceramic open-cell foams. The rheological behavior was explained on the bases of both porosity and actual powder density. It was proved that the use of multiple dippings fulfills flexibility requirements for washcoat load management. Multiple depositions with intermediate flash drying steps at 350 °C were carried out. Washcoat loads in the 2.5 to 22 wt. % range were obtained. Pore clogging was seldom observed in a limited extent in samples with high loading (>20 wt. %). Adhesion, evaluated by means of accelerated stress test in ultrasound bath, pointed out good results of all the deposited layers.

Keywords: ceramic open-cell foams; washcoat; catalyst deposition; rheology; structured support

1. Introduction

Structured catalysts and reactors for process intensification are receiving a large interest from the modern chemical engineering community [1]. A structured catalyst is intended as a continuum metallic or ceramic geometrical matrix (support) where voids (*i.e.*, channels) are present. The catalytically active phases are properly dispersed onto the support surface by direct incorporation or coating deposition. The latter is the most used technique, due to its simplicity and versatility [2]. Commonly, the deposited washcoat consists of a high surface area carrier, generally ceramic, where the metal active phase is properly dispersed. A variety of materials have been investigated as high surface area ceramic supports, such as alumina, silica, titania, and ceria [3–6]. In some process applications, low surface area catalysts have been investigated instead of high surface area ones. As an example, cerium oxide has been proposed as an active phase carrier, due to its oxygen storage properties [7]. Unfortunately, cerium oxide undergoes a fast surface area decrease when it is treated at high temperature [8]. Moreover, in several cases, this transition to lower surface area values occurs at temperatures that are lower than process operative conditions. Thus, in many cases, low surface area cerium-based catalysts need to be deposited onto structured supports [9].

The active phase usually consists of metal ions, and it is the core of the catalysis process. A variety of metals have been proposed in view of the different chemical processes. Among others, cobalt [10,11] and nickel [12,13] have been chosen because of their catalytic activity in many different reactions. Moreover, they have been proposed as a low cost and effective alternative to noble metals.

A variety of geometrical supports are now commercially available for catalytic purposes. They mainly differ for the structural and physical properties, such as chemical nature, surface area per unit volume or mechanical properties. Three way catalysts (TWCs) are one of the most diffused and investigated applications of structured supports to catalysis [14] because they are extensively used for gas pollution control in vehicle exhaust [15].

Among the different supports, solid open-cell foams are highly promising. Open-cell foams are characterized by a high interface area and high porosity, which could result in lower pressure drops and higher energy efficiency [16–18]. Due to their geometrical structure, high performance in terms of fluid/solid mass transfer are guaranteed.

As already reported, structured catalyst preparation is usually based on coating deposition onto the geometrical support surface. Depending on the structured substrate geometry, several deposition techniques for the catalytic thin layer have been made up [19,20]. Among them, dip-coating technique is the simplest, most versatile and cheapest one to be used in industrial practice. Moreover, dip-coating deposition can be easily applied to both metallic and ceramic supports of a variety of shapes [21].

The first step in dip-coating technique consists of the preparation of a slurry that is composed of a liquid phase in which the final powder to be deposited has to be suspended or better, dispersed. Then, the structured support is dipped in the liquid medium in order to fill the voids with a catalytic slurry precursor. Finally, the geometrical support is withdrawn from the slurry at a controlled rate. Depending on viscosity and support geometry, excess liquid removal is guaranteed by the opposite forces acting on the liquid during the withdrawal step. As a result, coating thickness depends on the balance between gravitational force, which promotes the removal of the liquid phase, and the viscous forces acting in the slurry, which involve the sliding resistance [22,23]. Therefore, the control of the coated layer properties,

i.e., thickness and adhesion, are mainly ruled by the slurry rheological behavior and the withdrawal velocity. As far as rheological behavior is concerned, the suspension formulation (e.g., water/powder ratio, acid/powder ration, and surfactant content) can be easily tuned in order to achieve the desired viscosity at the typically applied dip coating shear rates [21]. Indeed, at low viscosity values, which promote good adhesion, lower coating loads are obtained. On the other hand, when a higher viscosity is applied, the higher coating load obtained is counterbalanced by poor adhesion, and sometimes a few difficulties are faced in applying the method [24].

Different methods are available for both powder suspension (or dispersion) and slurry stabilization. A well-known method is based on the generation of electrostatic repulsions among the powder particles, promoted by the surface charging of the material to be dispersed in an acidic environment [24–26]. This procedure has been applied with success to high surface area powders, as their surface can be easily charged simply by managing the pH of the suspension. Unfortunately, this route is not easily applicable in the case of powders with low surface area, those characterized by chemical un-reactivity, or in the case of a possible dissolution of components. In all of these cases, an acid-free dispersion method needs to be used, and the selection of an alternative dispersant agent is required. Generally speaking, in the acid-free method organic molecules, more typically macromolecules, are used as dispersants. They are dissolved into the liquid phase so they can closely interact with the powder surface, allowing particle dispersion and slurry stabilization [27–29]. Many papers are reported in the literature regarding formulation and its effect on resulting slurries [30–32]. However, to our knowledge, fewer works have been reported on the production of slurries for coating deposition, via dipping, of low surface area powders onto open cell foams. In particular, scarce information is reported on the effect of the different dispersants and the composition of the final slurry properties. This study is of fundamental importance to correlate easily tunable experimental parameters, such as ratios between the components, with the rheological behavior of the slurry. Indeed, rheology is the main operative parameter to drive the final coating load, thickness, and adhesion, *i.e.*, which are the parameters of interest for industrial application [33].

Accordingly, the aim of this work is to clarify these aspects by studying the formulations and the procedures to deposit thin active layers of low surface area model catalyst powder, such as Ni- or Co-supported, onto low surface area ZrO_2. The catalytically active powders were produced by means of the incipient wetness impregnation technique using a commercial support. Different acid-free formulations based on water (H), glycerol (G), and polyvinyl alcohol (PVA) were studied, and the effect of the components that determine the slurry rheology was assessed. The different slurries were tested to coat 30 PPI (Pores Per Inch) ceramic open-cell foams via the dip-coating technique. A correlation among the final coating load, thickness, and adhesion after thermal treatments with the slurry composition and rheology was proposed. An attempt to rationalize the rheological behavior at the light of composition was also made.

2. Results and Discussion

2.1. Catalyst Characterization

Catalytic powders characterization is reported in Figure 1 and Table 1. For the sake of comparison, the characterization of the pristine morphological carrier (ZrO_2) is also reported.

XRD patterns (Figure 1) clearly showed the reflections of the monoclinic ZrO_2 support. Additional reflections at 37.2°, 43.2° and 63° 2θ can be clearly seen in case of the Ni-containing sample; the latter were attributed to NiO, while the one that was detected at 36.9° in the Co-based sample was attributed to Co_3O_4.

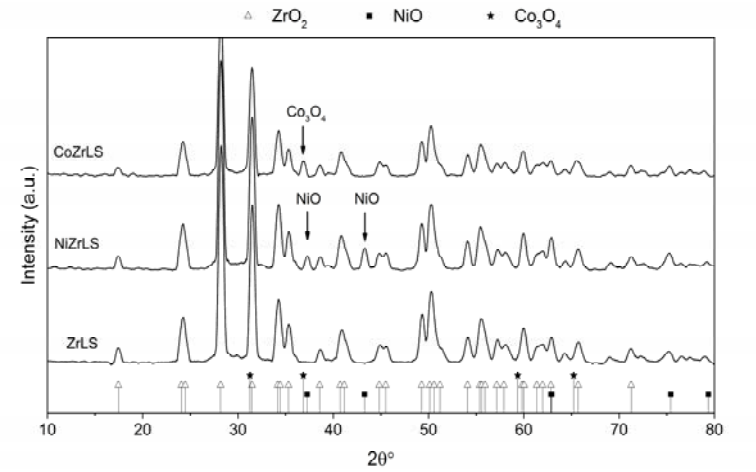

Figure 1. XRD spectra of the impregnated powders.

Table 1. Morphological characterization of the powders.

Sample	Active Phase Crystal Size (nm) (by XRD)	Surface Area ($m^2 \cdot g^{-1}$)	Pore Volume ($cm^3 \cdot g^{-1}$)
ZrLS	-	27	0.2
NiZrLS	28	14	0.1
CoZrLS	25	19	0.1

The crystallite dimensions of the carrier and the active phase, which were calculated according to Scherrer equation, were in the range of 25–28 nm, thus, almost comparable.

Regarding morphology, very close surface areas and pores volumes were measured for the active materials: a decrease of the surface area was observed upon impregnation that was accompanied by a decrease of the pore volumes. This effect is clearly explained by the partial occupation of pores due to the presence of the active phase.

According to the procedure reported in the experimental section, all the powders, carrier and active materials were dispersed in the HGP liquid medium, and their rheological behaviors were compared. Results are reported in Figure 2.

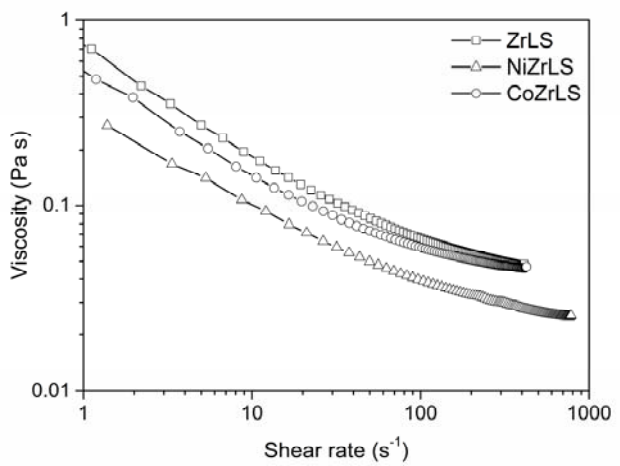

Figure 2. Rheological behavior of zirconia-based slurries.

Apparently, active phase presence did not affect rheological properties. Indeed, shear thinning behaviors were found for all the samples. In order to get information on the non-Newtonianity degree of the slurries, the flow curves slope was determined in the 10–100 s^{-1} shear rate range. Generally speaking, higher slope values (in modulus) correspond to a more marked shear thinning behavior. For all samples, slopes in the range of 0.6–0.4 were calculated; this highlighted a very close rheological behavior for the three slurries. The powder composition exerted a different effect, since the presence of the active phase induced lower viscosity values in all the shear rate range (Figure 2). Such differences cannot be directly related neither to the surface area nor to the porosity due to the close values of these parameters detected for the three samples; similar considerations can be done for the active phase content, too. On the contrary, the absolute viscosity appeared to be much more specific for the metal cations present at the carrier surface. The effect of the presence of an active phase onto the carrier surface was already reported in the literature [34]. Accordingly, the modification of the surface nature was reported as responsible for a different powder-dispersant interaction, which influenced the rheological behavior. However, in this case, this effect should be quite peculiar considering the strong chemical similarity between Ni and Co both in terms of atomic weight and atomic number.

Accordingly, an attempt to rationalize the viscosity behavior was done, considering properties other than those mentioned above or a combination of properties reported so far.

A possible explanation for the rheological behavior could be found by considering the actual volume fraction of the powders. To evaluate this aspect, a representative model to describe the powders has to be built. In the model, three components were considered: (1) powder nature (mainly related to the molar weight); (2) powder density (mainly related to porosity); and (3) powder size and size distribution.

The first consideration regarded the composition of the different powders, since slurries formulation was obtained by considering the powders content on mass base. The presence of the active phase in its oxidized form should be taken into account, since it affects the powder molar weight and consequently, the powder concentration in the slurry. In order to quantify this effect, the actual amount of the active phase (in the oxidized form ($m_{\mathrm{Ox.Act.Ph}}$)) was determined according to Equation (1)

$$m_{Ox.Act.Ph} = \frac{m_{Met.Act.Ph}}{M_{MetalIon}} \frac{(g)}{\left(\frac{g}{mol}\right)} \cdot M_{Ox}\left(\frac{g}{mol}\right) \quad (1)$$

where $m_{\text{Met.Act.Ph}}$ (g) is the mass of the active phase (metallic form), M_{MetalIon} is the atomic mass of the metal ion and M_{Ox} the molecular weight of the active phase (oxidized form). Starting from Equation (1), support weight fraction was recalculated according to Equation (2).

$$K = \frac{m_{\text{sup port}}}{m_{\text{sup port}} + m_{Ox.Act.Ph}} \tag{2}$$

K equals to one for the bare support, while it is lower than one for the active powders (Table 2). However, *K* cannot completely describe the powders because no powder density was taken into account in Equation (1). Powder density is directly correlated to the morphological properties and particularly to porosity that can be evaluated by means of BET analysis. Therefore, in order to properly evaluate the actual density of the powders, crystallographic density and sample porosity were introduced in the calculation. In the case of active powders, crystallographic density was assumed as the average of the densities of all the phases, weighted by composition as reported in Equation (3):

$$\rho_{bulk} = \sum_{i=1}^{N.C.} \%wt._i \cdot \rho_{bulk,i}, \text{ with } \%wt._i = \frac{m_i}{m_{\text{sup port}} + m_{m_{Ox.Act.Ph}}} \tag{3}$$

where "*i*" is the any phase present in the powder in the oxidized form. The "real" density was thus calculated by taking into account the evaluated material porosity. Porosity values were used to determine the powder void fraction (φ) and, thus, the real powder density (ρ_{real}) calculated according to Equation (4):

$$\rho_{real} = \rho_{bulk} \cdot (1 - \varphi), \text{ with } \varphi = \frac{V_p}{V_m} = \frac{\text{pore volume}}{\text{specific volume}} \tag{4}$$

Moreover, to give a complete description of the powders and to evaluate their actual concentration in the slurry, the particle size and size distribution, evaluated by granulometric analysis, were introduced in the model. Accordingly, the weighted volumetric fraction was calculated by Equation (5):

$$V_{Fract} = \sum_{i=1}^{D_P} V_i \cdot \text{Percentage}_i \tag{5}$$

where V_{fract} is the volume of the particle (V_i) and Percentage_i is the relative amount of particles with the *i*-th diameter. For volume calculation, a spherical shape was assumed for particles while the specific volume was assumed as equal to the reciprocal of density. Finally, the number of particles per unit volume was obtained by using Equation (6)

$$\text{Particles concentration} = \frac{m_{powder}}{\rho_{real} \cdot V_{Fract} \cdot V_{liq}} \tag{6}$$

where ρ_{real} is the real density of powder and V_{liq} is the volume of dispersing HGP liquid medium. Results are reported in Table 2.

Table 2. Powder physical properties and slurry viscosity values.

Powder	K	Bulk Density ($g \cdot cm^{-3}$)	Real Density ($g \cdot cm^{-3}$)	Particles Concentration (Particles cm^{-3})	Viscosity (Pa·s) at Shear Rate:		
					1 s^{-1}	10 s^{-1}	100 s^{-1}
ZrLS	1	5.68	1.13	1.50×10^8	0.743	0.185	0.067
NiZrLS	0.91	5.77	2.43	4.24×10^7	0.309	0.1	0.04
CoZrLS	0.76	5.78	2.16	4.10×10^7	0.532	0.14	0.059

On these bases, viscosity at three selected shear rates was plotted as a function of powder density (Figure 3).

Viscosity was found to decrease linearly as powder density increased. Once the mass of powder to be dispersed is fixed, a larger material density results in a lower number of particles per volume unit. The number of particles per volume unit directly influences the rheological behavior: a higher number of particles leads to higher viscosity values [35,36]. Thus, the rheological slurry behavior can be explained on these bases. Pure ZrO_2 (the carrier), which is a less dense material than the impregnated one, showed the highest viscosity because the same powder amount (weight base) had a larger number of particles present. When powder density increases, such as in the case of the active powders, the number of particles decreases; therefore, powder concentration and slurry viscosity also decreases.

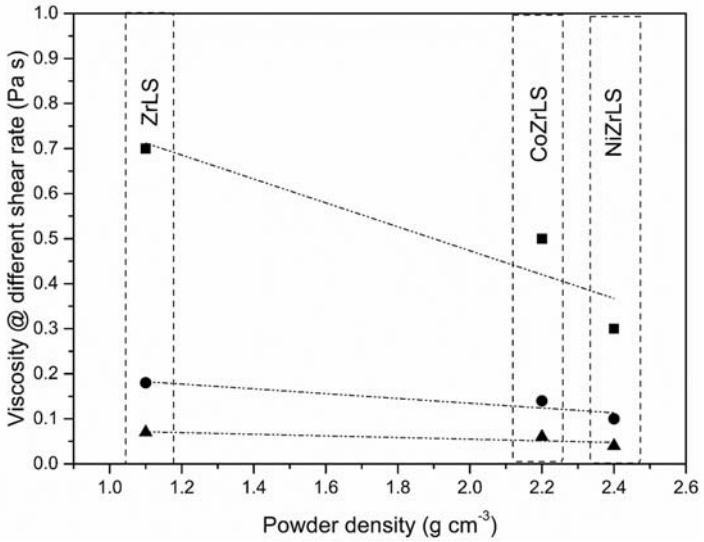

Figure 3. Viscosity at three selected shear rates as the function of the powder density (triangles: SR 100 s^{-1}; circles: SR 10 s^{-1}; squares: SR 1 s^{-1}).

This picture was confirmed by plotting the viscosity as a function of the particle concentration, which was calculated as reported above (Figure 4). At any shear rate, the viscosity increases with the particles concentration. Results of Figure 4 are in line with the conventional behavior of slurry viscosity. It is well known that the viscosity of concentrated dispersions is higher than that of diluted ones. This effect may be related with an increase of particle-particle interaction. Moreover, the fact that parallel lines were found suggested the presence of the same interaction mechanism at any shear rates.

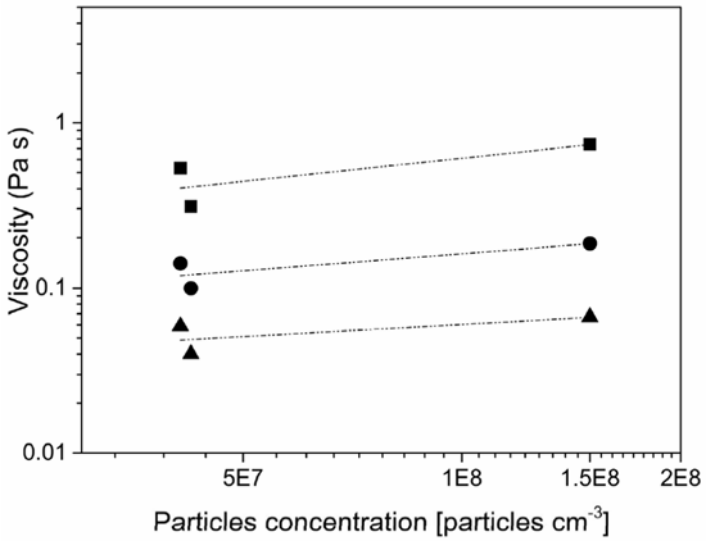

Figure 4. Viscosity as a function of particles concentration (triangles: SR 100 s^{-1}; circles: SR 10 s^{-1}; squares: SR 1 s^{-1}).

2.2. Washcoat Deposition

HGP-based slurries were deposited onto the 30 PPI ceramic foams via dip-coating process and then, thermally treated. Up to three multiple depositions were performed. It is well known that washcoat load, the parameter of interest, is correlated with viscosity, *i.e.*, the main operative variable of the process [37]. Accordingly, the coating load after calcination was plotted as a function of the viscosity values at shear rate $10 \cdot s^{-1}$, the one of interest for dip-coating application (Figure 5). Regardless slurry formulation, a quite linear load-viscosity correlation was found.

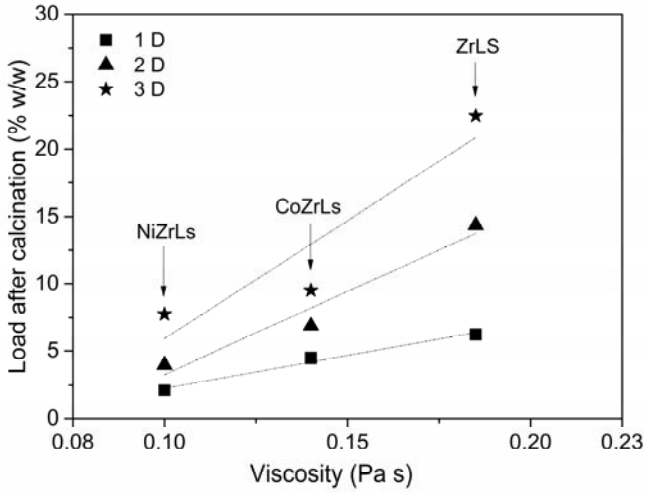

Figure 5. Coating Load as a function of viscosity and of the number of subsequent depositions.

As expected, the washcoat load increased with viscosity and was observed at any dipping number. Due to the highest viscosity values, the higher loads were obtained with the pristine ZrO_2 slurries which were found to reach approximately 22 wt. % after three dippings.

When more than one dipping was applied, the deposition seemed not to be affected by the presence of the previous washcoat layer. This effect is better evidenced when the washcoat load after calcination is plotted as a function of the dipping number (Figure 6).

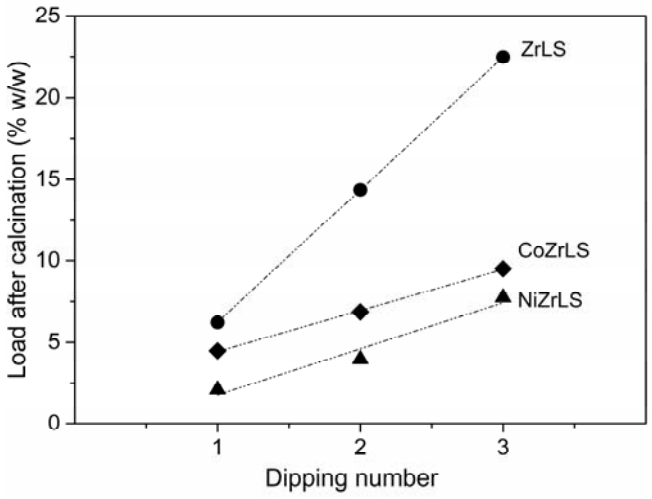

Figure 6. Coating load as a function of the dipping numbers.

A linear trend between load and dipping number was found, suggesting dipping number as a useful tool to manage washcoat load.

Results on adhesion tests—by means of an ultrasound stress test in petroleum ether—are shown in Figure 7.

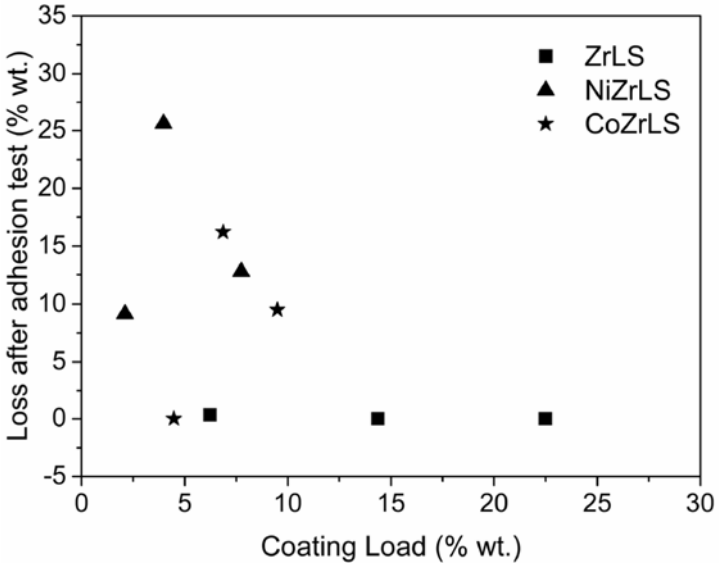

Figure 7. Weight loss after adhesion test for Zr-based samples as a function of load after calcination.

From the analysis of points of Figure 7, adhesion seemed strongly related to the coating composition; in the case of pure ZrO_2, negligible or no weight losses were present while the presence of active phase led to higher weight losses, with a relative maximum in correspondence of the intermediate washcoat load values. Generally speaking, higher washcoat load should determine higher losses after adhesion test, due to layer thickness. On the contrary, in these samples an overall increase of adhesion was found

with load increase. For the considered samples, the effect of the different surface composition should also be taken into account even though this effect cannot be easily evaluated. Anyway, due to the large complexity of the involved phenomena and to the brittleness of the support foam, this point deserves more study to be clarified.

A qualitative washcoat analysis as a function of dipping number was performed on the active powders by using an optical microscope (Figure 8).

Figure 8 shows the images after flash drying. As described in the experimental section, this step is performed at 350 °C for 6 min: these operative parameters are suitable for solvent removal, but they are not enough for the total decomposition of the organic components which is still incomplete [38]. To analyze the washcoat at this step can be highly useful: the partial decomposition of the organic compound will result in a darkening of the surface that should allow for a better vision of coating coverage and homogeneity. Both samples clearly showed a surface darkening that was qualitatively interpreted as a homogeneous distribution of the washcoat load. As a matter of fact, white areas, which correspond to the bare substrate, were still evident only after one dipping; then, they gradually decreased and tended to disappear upon multiple depositions. After three dippings, a good coverage was reached. Almost no pore clogging occurred: only limited pore clogging was found for the CoZrLS (left side in the picture).

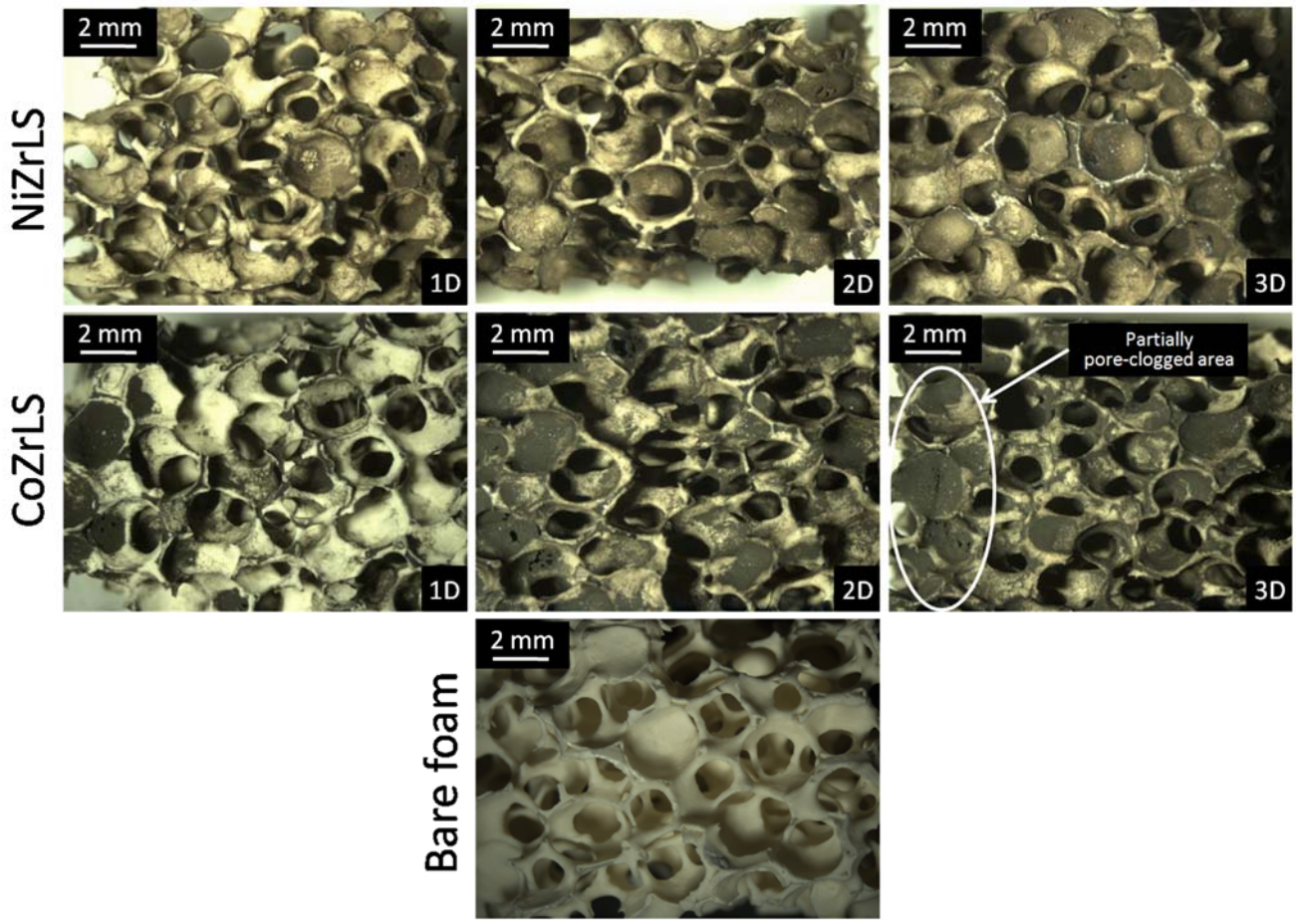

Figure 8. Optical images of NiZrLS (1D to3D) and CoZrLS (1D to3D) deposited on 30 PPI foams: effect of multiple dippings after flash drying. For the sake of comparison, an image of the bare foam has been added at the bottom of the image.

Figure 8 shows the images after flash drying. As described in the experimental section, this step is performed at 350 °C for 6 min: these operative parameters are suitable for solvent removal, but they are not enough for the total decomposition of the organic components which is still incomplete [38]. To analyze the washcoat at this step can be highly useful: the partial decomposition of the organic compound will result in a darkening of the surface that should allow for a better vision of coating coverage and homogeneity. Both samples clearly showed a surface darkening that was qualitatively interpreted as a homogeneous distribution of the washcoat load. As a matter of fact, white areas, which correspond to the bare substrate, were still evident only after one dipping; then, they gradually decreased and tended to disappear upon multiple depositions. After three dippings, a good coverage was reached. Almost no pore clogging occurred: only limited pore clogging was found for the CoZrLS (left side in the picture).

In order to evaluate the deposited layers at higher magnification, washcoat after calcination was analyzed by SEM measurements (Figure 9). The results after three dippings are reported for the active powders.

Acquisitions were performed in back scattering, and they once more demonstrated the good coverage homogeneity of the surface (Figure 9). Few defects were present, but they were of limited extent and localized. Coating surface, analyzed at higher magnification (Figure 9e,f), showed evidence of the presence of cracks of limited depth; another coating layer (not the bare support) was seen underneath.

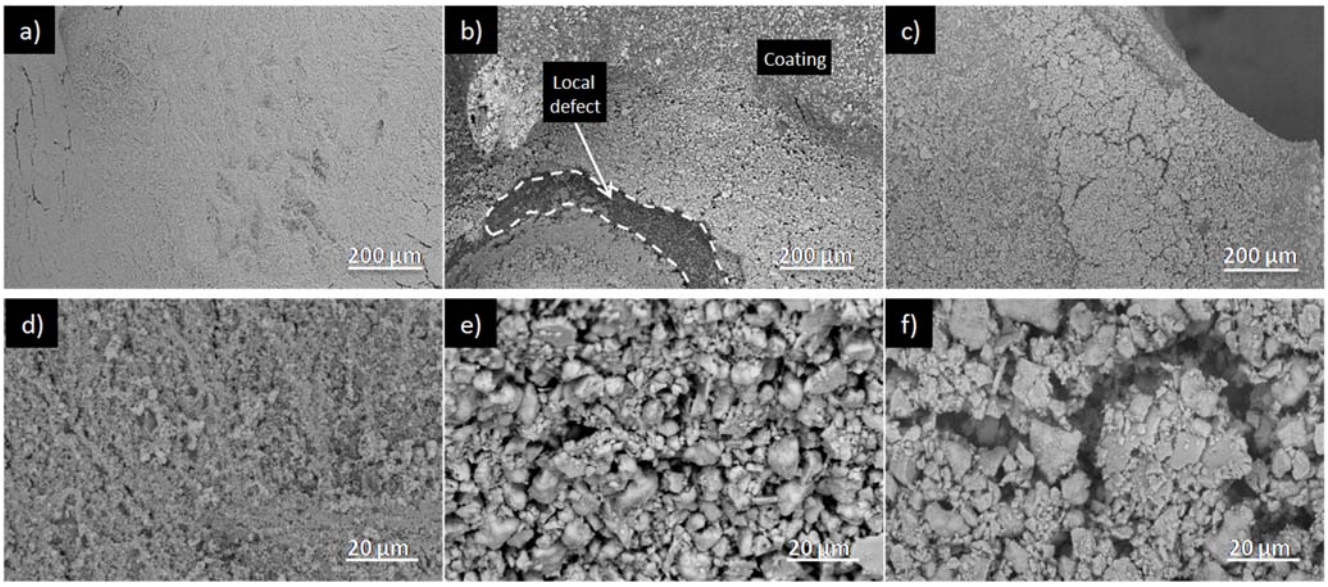

Figure 9. Back scattering SEM analysis of ZrLS, (**a**,**d**), NiZrLS (**b**,**e**) and CoZrLS (**c**,**f**) coated samples after three dippings at different magnifications (100X and 1000X).

3. Experimental Section

3.1. Catalytic Powders Preparation and Characterization

A commercially available low surface area carrier was used for catalyst production, namely zirconium oxide supplied by Melcat (in the following, ZrLS).

Catalysts were produced by using the incipient wetness impregnation method [19]. Nickel nitrate hexahydrate (98.5%, Sigma-Aldrich, St. Louis, MO, USA) and cobalt nitrate hexahydrate (98%,

Sigma-Aldrich, St. Louis, MO, USA) were used as nickel and cobalt active phases precursors, respectively. These metal salts were used to obtain a final load equal to 7 wt. %, on a metal base.

The precursors solution was wisely dropped onto the carrier. Impregnated powders were dried overnight at 120 °C, and then, they were calcinated in order to decompose the nitrate precursors and to obtain the final oxide. In particular, Co-based samples were calcinated at 400 °C while Ni-based samples were treated at 800 °C; in both cases, dwell was set at 10 h, with heating and cooling rate of 2 °C·min^{-1}. The two different calcination temperatures were chosen in accordance with possible catalytic applications (*i.e.*, Oxy-Steam Reforming for Ni-based catalysts [39] and Fisher Tropsch synthesis for Co-bases samples [11]. A final metal load about 10 wt. % was measured for all powders.

Impregnated powders were characterized by means of X-ray diffraction. A D8 Advance diffractometer (Bruker, Billerica, MA, USA) and a Cu-K$_\alpha$ radiation were used (10–80° 2θ range, 40 kV and 40 mA, step scan 0.02° 2θ, time 1 s·step^{-1}). Crystallite dimensions were evaluated from the reflection line broadening (FWHM, calculated by Topas) using the Scherrer equation [40].

The powders particle size was evaluated by using a CILAS 1180 laser granulometer (Compagnie Industrielle des Lasers, Orleans, France).

BET surface area and pore volume were determined by N_2 adsorption and Hg intrusion; in the first case, a Tristar 3000 device was used (Micromeritics, Norcross, GA, USA). N_2 physisorprion measurements were carried out after heating at 150 °C overnight, under vacuum. An Autopore IV instrument (Micromeritics, Norcross, GA, USA) was used for Hg intrusion.

3.2. Washcoating

The powders dispersion formulation is based on a dispersant, glycerol (G) (87% *w*/*w* water solution, Sigma-Aldrich, St. Louis, MO, USA), a solvent/diluent, distilled water (H), and a rheology modifier, polyvinyl alcohol (PVA) (Mowiol, Sigma-Aldrich, St. Louis, MO, USA). Weight ratios among the three components were calculated with respect to the powders (PW), and they were respectively set at: G/PW = 1.9, H/PW = 1.8 and PVA/PW = 0.07. In the following, the liquid medium based on this formulation will be labeled as HGP.

The slurry was obtained by means of a procedure reported elsewhere [24]. Briefly, in a typical experiment, PVA was dissolved in distilled water at 85 °C; then glycerol was added, always under magnetic stirring. The obtained HGP liquid medium was used to disperse catalyst powders. The powder was added to the HGP solution, and the resulting slurry was ball-milled for 24 h (50 rpm of rotation rate) in a polyethylene jar using ZrO_2 spheres as grinding bodies. After the milling process, a sonication pre-treatment was performed for 30 min on the slurries in order to reduce foaming.

The slurries rheological behavior was evaluated in the 1–10^3 s^{-1} shear rate range by means of a DSR 200 instrument (Rheometrics, New Castle, DE, USA) by using the parallel plates geometry and plates of 40 mm of diameter.

Before coating deposition, supports were cleaned with acetone for 30 min in an ultrasound bath.

Slurries were deposited on Yttria-stabilized Zirconia Alumina (YZA) open-cell foams (Selee Company, Hendersonville, NC, USA), with a nominal pore density of 30 PPI (pore per inch). Structured supports were cut in parallelepiped shape with squared section; dimensions were set at 1.5 cm and 1 cm for length and section, respectively.

Dip-coating was used as the deposition technique. Both the dipping and withdrawal rate were set at 13 ($cm \cdot min^{-1}$). After the dipping step, coated samples were flash dried [38] for 6 min at 350 °C in a sealed oven. Then, a final calcination thermal treatment was performed for 10 h at 400 °C and 800 °C for Co- and Ni-based materials respectively; in both cases, dwell was set at 10 h with a heating and cooling rate of 2 $°C \cdot min^{-1}$. When necessary, multiple depositions were performed; the dipping procedure was repeated, and flash drying was performed between two subsequent dippings.

Washcoat load was evaluated by the weight difference of bare and coated foam.

Coated layers homogeneity and morphology were evaluated by means of optical (SZ-CTV microscope, Olympus, Tokio, Japan) and scanning electronic microscopy (Stereoscan 360, Cambridge Instruments microscope, Somerville, MA, USA).

Coating adhesion was determined by coated samples sonication for 30 min in a petroleum ether bath, according to literature [34]. In Figure 10, a schematic representation of a typical procedure for structured catalyst production is reported.

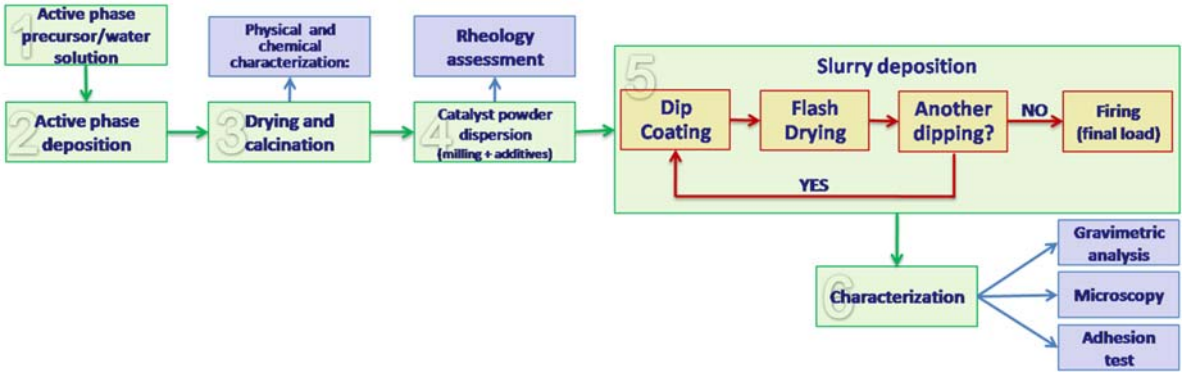

Figure 10. Scheme for catalyst production and washcoat deposition (slurry composition and details of the procedures as reported above).

4. Conclusions

(1) The use of an acid-free water-based formulation proved to be effective for the dispersion of model catalytic powders characterized by low surface areas. The obtained slurries are suitable for deposition on ceramic open cell foams via dip-coating.

(2) A dependence between the powder properties and the final rheology was evidenced. In particular, the rheological behavior, being directly related to both powder particles porosity and density, could be managed by taking into account these properties during formulation. Active phase presence influences particles properties, although present in a limited amount.

(3) From a practical point of view, chemical composition (*i.e.*, molar weight) and porosity were found to be simple and detectable parameters to be used in slurry formulation to control the rheological behavior.

(4) The use of multiple dippings proved to fulfill the flexibility requirements for washcoat load management. All the formulations obtained good results in terms of washcoat load and adhesion. Local and limited pore clogging occurred only in the washcoat at very high load degree (higher than 20 wt. %).

(5) Depending on the powder to be deposited and on the operative condition, promising results have been obtained in terms of adhesion. Most samples displayed losses lower than 10 wt. %, which was reported in literature as satisfactory for washcoat adhesion on open-cell foams [38].

(6) Although, up to now an "*a priori*" formulation of the slurry is hardly to be obtained without any experimental base, the results here reported can help to reduce experimental tests in a trial-and-error approach.

Acknowledgments

This work was funded by the Ministry of Education, University and Research, Italy (MIUR, Progetti di Ricerca Scientifica di Rilevante Interesse Nazionale 2010–2011) within the project IFOAMS ("Intensification of catalytic processes for clean energy, low-emission transport and sustainable chemistry using open cell FOAMS as novel advanced structured materials", protocol no. 2010XFT2BB).

Author Contributions

R.B. and C.C. conceived and designed the experiments. M.C. and F.P. performed the experiments; R.B., M.C., F.P. and C.C. analyzed the data; C.C. contributed reagents/materials/analysis tools; R.B. and C.C. wrote the paper.

Conflicts of Interest

The authors declare no conflict of interest.

References

1. Tronconi, E.; Groppi, G. Preface. *Catal. Today* **2009**, *147*, S1.
2. Montebelli, A.; Visconti, C.G.; Groppi, G.; Tronconi, E.; Cristiani, C.; Ferreira, C.; Kohler, S. Methods for the catalytic activation of metallic structured substrates. *Catal. Sci. Tech.* **2014**, *4*, 2846–2870.
3. Bagheri, S.; Muhd Julkapli, N.; Bee Abd Hamid, S. Titanium dioxide as a catalyst support in heterogeneous catalysis. *Sci. World J.* **2014**, *2014*, 727496.
4. Huirache-Acuna, R.; Nava, R.; Peza-Ledesma, C.L.; Lara-Romero, J.; Alonso-Nunez, G.; Pawelec, B.; Rivera-Munoz, E.M. SBA-15 mesoporous silica as catalytic support for hydrodesulfurization catalysts—Review. *Materials* **2013**, *6*, 4139–4167.
5. Trueba, M.; Trasatti, S.P. γ-Alumina as a support for catalysts: A review of fundamental aspects. *Eur. J. Inorg. Chem.* **2005**, *17*, 3393–3403.
6. Maciel, C.G.; Silva, T.D.; Hirooka, M.I.; Belgacem, M.N.; Assaf, J.M. Effect of nature of ceria support in CuO/CeO_2 catalyst for PrO_x-CO reaction. *Fuel* **2012**, *97*, 245–252.
7. Maupin, I.; Mijoin, J.; Barbier, J.; Bion, N.; Belin, T.; Magnoux, P. Improved oxygen storage capacity on CeO_2/zeolite hybrid catalysts. Application to VOCs catalytic combustion. *Catal. Today* **2011**, *176*, 103–109.
8. Periyat, P.; Laffir, F.; Tofail, S.A.M.; Magner, E. A facile aqueous sol-gel method for high surface area nanocrystalline CeO_2. *RSC Adv.* **2011**, *1*, 1794–1798.

9. Pino, L.; Vita, A.; Laganà, M.; Recupero, V. Hydrogen from biogas: Catalytic *tri*-reforming process with Ni/La-Ce-O mixed oxides. *Appl. Catal. B* **2014**, *148–149*, 91–105.
10. Iglesia, E. Design, synthesis, and use of cobalt-based Fischer-Tropsch synthesis catalysts. *Appl. Catal. A* **1997**, *161*, 59–78.
11. Khodakov, A.Y.; Chu, W.; Fongarland, P. Advances in the development of novel cobalt Fischer-Tropsch catalysts for synthesis of long-chain hydrocarbons and clean fuels. *Chem. Rev.* **2007**, *107*, 1692–1744.
12. Wang, C.M.; Friedrich, S.; Younkin, T.R.; Li, R.T.; Grubbs, R.H.; Bansleben, D.A.; Day, M.W. Neutral nickel(II)-based catalysts for ethylene polymerization. *Organometallics* **1998**, *17*, 3149–3151.
13. Li, Y.D.; Li, D.X.; Wang, G.W. Methane decomposition to CO_x-free hydrogen and nano-carbon material on group 8–10 base metal catalysts: A review. *Catal. Today* **2011**, *162*, 1–48.
14. Matsumoto, S.I. Recent advances in automobile exhaust catalysts. *Catal. Today* **2004**, *90*, 183–190.
15. Koltsakis, G.C.; Stamatelos, A.M. Catalytic automotive exhaust aftertreatment. *Prog. Energy Combust. Sci.* **1997**, *23*, 1–39.
16. Ghosh, I. Heat transfer correlation for high-porosity open-cell foam. *Int. J. Heat Mass Transf.* **2009**, *52*, 1488–1494.
17. Giani, L.; Groppi, G.; Tronconi, E. Mass-transfer characterization of metallic foams as supports for structured catalysts. *Ind. Eng. Chem. Res.* **2005**, *44*, 4993–5002.
18. Giani, L.; Groppi, G.; Tronconi, E. Heat transfer characterization of metallic foams. *Ind. Eng. Chem. Res.* **2005**, *44*, 9078–9085.
19. Campanati, M.; Fornasari, G.; Vaccari, A. Fundamentals in the preparation of heterogeneous catalysts. *Catal. Today* **2003**, *77*, 299–314.
20. Meille, V. Review on methods to deposit catalysts on structured surfaces. *Appl. Catal. A* **2006**, *315*, 1–17.
21. Avila, P.; Montes, M.; Miro, E.E. Monolithic reactors for environmental applications—A review on preparation technologies. *Chem. Eng. J.* **2005**, *109*, 11–36.
22. Brinker, C.J.; Scherer, G.W. *Sol-Gel Science*; Academic Press: San Diego, CA, USA, 1990.
23. Middleman, S. *Fundamentals of Polymers Processing*; McGraw-Hill Companies: New York, NY, USA, 1977; p. 448.
24. Valentini, M.; Groppi, G.; Cristiani, C.; Levi, M.; Tronconi, E.; Forzatti, P. The deposition of γ-Al_2O_3 layers on ceramic and metallic supports for the preparation of structured catalysts. *Catal. Today* **2001**, *69*, 307–314.
25. Visconti, C.G.; Tronconi, E.; Lietti, L.; Groppi, G.; Forzatti, P.; Cristiani, C.; Zennaro, R.; Rossini, S. An experimental investigation of Fischer-Tropsch synthesis over washcoated metallic structured supports. *Appl. Catal. A* **2009**, *370*, 93–101.
26. Cristiani, C.; Visconti, C.G.; Finocchio, E.; Stampino, P.G.; Forzatti, P. Towards the rationalization of the washcoating process conditions. *Catal. Today* **2009**, *147*, S24–S29.
27. Phan, X.K.; Bakhtiary-Davijany, H.; Myrstad, R.; Pfeifer, P.; Venvik, H.J.; Holmen, A. Preparation and performance of Cu-based monoliths for methanol synthesis. *Appl. Catal. A* **2011**, *405*, 1–7.
28. Won, J.Y.; Jun, H.K.; Jeon, M.K.; Woo, S.I. Performance of microchannel reactor combined with combustor for methanol steam reforming. *Catal. Today* **2006**, *111*, 158–163.

29. Germani, G.; Stefanescu, A.; Schuurman, Y.; van Veen, A.C. Preparation and characterization of porous alumina-based catalyst coatings in microchannels. *Chem. Eng. Sci.* **2007**, *62*, 5084–5091.
30. Lin, K.S.; Pan, C.Y.; Chowdhury, S.; Lu, W.; Yeh, C.T. Synthesis and characterization of $CuO/ZnO\text{-}Al_2O_3$ catalyst washcoat thin films with ZrO_2 sols for steam reforming of methanol in a microreactor. *Thin Solid Films* **2011**, *519*, 4681–4686.
31. Barth, N.; Zimmermann, M.; Becker, A.E.; Graumann, T.; Garnweitner, G.; Kwade, A. Influence of TiO_2 nanoparticle synthesis on the properties of thin coatings. *Thin Solid Films* **2015**, *574*, 20–27.
32. Truyen, D.; Courty, M.; Alphonse, P.; Ansart, F. Catalytic coatings on stainless steel prepared by sol-gel route. *Thin Solid Films* **2006**, *495*, 257–261.
33. Agrafiotis, C.; Tsetsekou, A.; Leon, I. Effect of slurry rheological properties on the coating of ceramic honeycombs with yttria-stabilized-zirconia washcoats. *J. Am. Ceram. Soc.* **2000**, *83*, 1033–1038.
34. Cristiani, C.; Finocchio, E.; Latorrata, S.; Visconti, C.G.; Bianchi, E.; Tronconi, E.; Groppi, G.; Pollesel, P. Activation of metallic open-cell foams via washcoat deposition of $Ni/MgAl_2O_4$ catalysts for steam reforming reaction. *Catal. Today* **2012**, *197*, 256–264.
35. Olhero, S.M.; Ferreira, J.M.F. Influence of particle size distribution on rheology and particle packing of silica-based suspensions. *Powder Technol.* **2004**, *139*, 69–75.
36. Zupancic, A.; Lapasin, R.; Kristoffersson, A. Influence of particle concentration on rheological properties of aqueous $\alpha\text{-}Al_2O_3$ suspensions. *J. Eur. Ceram. Soc.* **1998**, *18*, 467–477.
37. Agrafiotis, C.; Tsetsekou, A. The effect of processing parameters on the properties of γ-alumina washcoats deposited on ceramic honeycombs. *J Mater. Sci.* **2000**, *35*, 951–960.
38. Balzarotti, R.; Cristiani, C.; Latorrata, S.; Migliavacca, A. Washcoating of low surface area cerium oxide on complex geometry substrates. *Part. Sci. Technol.* **2015**, in press.
39. Sutton, D.; Kelleher, B.; Ross, J.R.H. Review of literature on catalysts for biomass gasification. *Fuel Process. Technol.* **2001**, *73*, 155–173.
40. Cullity, B.D.; Stock, S.R. *Elements of X-ray Diffraction*, 3rd ed.; Prentice Hall: Upper Saddle River, NJ, USA, 2001.